IJARSCT
International Journal of Advanced Research in Science, Communication and Technology
International Open-Access, Double-Blind, Peer-Reviewed, Refereed, Multidisciplinary Online Journal
ISSN: 2581-9429
Volume 6, Issue 6, June 2026
Impact Factor: 8.2

Structural Health Monitoring Using Various Types of Sensors: Principles, Architectures, and AI-Integrated Analytics

Ashutosh Ramesh Dighe[1], Avanti Santosh Gawali[2], Sakshi Sanjay Dawkhar[3], Nikita Baburao Jadhav[4], Dr. S. B. Kandekar[5]
[1,2,3,4]Department of Civil Engineering
[5]Department of Civil Engineering (Supervisor)
Amrutvahini College of Engineering, Sangamner, Maharashtra, India

Abstract: *Structural Health Monitoring (SHM) has emerged as a transformative paradigm in modern infrastructure management, enabling continuous real-time assessment of the integrity and performance of civil, mechanical, and aerospace structures. This paper presents a comprehensive review and technical analysis of SHM systems that employ diverse sensor modalities—including strain gauges, accelerometers, fiber-optic sensors, piezoelectric transducers, microelectromechanical systems (MEMS), ultrasonic probes, temperature sensors, displacement sensors, vibration sensors, and wireless smart sensors. Each sensor category is examined with respect to its operating principle, sensitivity, accuracy, power budget, and suitability for specific structural applications such as bridges, dams, railways, wind turbines, high-rise buildings, and aircraft frames. The paper further elaborates the end-to-end SHM system architecture, covering data-acquisition hardware, signal-conditioning circuits, wireless communication protocols, cloud/IoT integration, and real-time monitoring dashboards. A dedicated methodology section for-malizes signal-processing pipelines, feature extraction strategies, and damage-detection algorithms, with emphasis on machine-learning and deep-learning models including Long Short-Term Memory (LSTM) networks and Convolutional Neural Networks (CNNs). A novelty contribution of this work is the proposal of an Integrated Multi-Sensor Fusion Framework with AI-Based Analytics that merges heterogeneous sensor streams to improve damage-localization accuracy beyond what any single sensor can achieve. Comparative tables and performance discussions highlight cost-accuracy trade-offs, environmental robustness, and deployment feasibility. Challenges such as sensor drift, environmental noise, power constraints, and cybersecurity vulnerabilities are critically evaluated. Finally, future directions involving digital twins, edge AI, energy harvesting, and 6G-enabled SHM ecosystems are identified.*

Keywords: Structural Health Monitoring, SHM, Sensor Fusion, IoT, MEMS, Fiber Optic Sensors, Piezoelectric, Accelerom-eter, Machine Learning, Digital Twin, Damage Detection, Wireless Sensor Networks

I. INTRODUCTION

A. Definition of Structural Health Monitoring

Structural Health Monitoring (SHM) is defined as the process of implementing a damage-identification and characterization strategy for engineering structures through the integration of sensors, data-acquisition systems, and signal-processing algorithms [1]. In its broadest form, SHM encompasses damage detection, localization, classification, and quantification, with the ultimate objective of estimating the remaining service life of a structure [2]. The concept

IJARSCT
International Journal of Advanced Research in Science, Communication and Technology
International Open-Access, Double-Blind, Peer-Reviewed, Refereed, Multidisciplinary Online Journal
ISSN: 2581-9429
Volume 6, Issue 6, June 2026
Impact Factor: 8.2

draws from the fields of structural dynamics, non-destructive evaluation (NDE), mechatronics, and computer science to form an interdisciplinary discipline capable of generating actionable intelligence from structural data.

B. Importance Across Engineering Domains

The global infrastructure portfolio—comprising more than 900,000 bridges in the United States alone, millions of kilometers of railway track, thousands of offshore wind turbines, and a rapidly expanding fleet of commercial aircraft—faces mounting pressures from aging, climate-induced stress, and rising operational demands [3]. In the civil domain, SHM enables engineers to quantify load-induced deformations, detect fatigue cracks in steel girders, and monitor settlement in concrete foundations. In mechanical and industrial contexts, SHM reduces unplanned downtime in rotating machinery. In aerospace, real-time SHM data informs maintenance decisions critical for passenger safety. Within the broader paradigm of smart infrastructure, SHM serves as the nervous system of intelligent buildings, continuously relaying data to building management systems and digital-twin platforms [4].

C. Need for Continuous Monitoring and Predictive Maintenance

Traditional inspection regimes are inherently reactive and incapable of detecting the onset of progressive structural degradation between inspection cycles. A seminal example is the 2007 collapse of the I-35W Mississippi River Bridge, where fatigue-induced gusset-plate failure remained undetected prior to the catastrophic event [5]. Continuous SHM shifts the maintenance paradigm from corrective and time-based preven-tive strategies to predictive maintenance, in which deterioration trends are identified early, maintenance is scheduled at optimal intervals, and structural reserves are exploited safely.

II. LITERATURE REVIEW

A. Historical Context and Traditional Techniques

Early SHM research in the 1970s and 1980s focused primarily on offshore oil-platform monitoring using accelerom-eters to detect changes in natural frequencies caused by damage [6]. These vibration-based methods, rooted in modal analysis, became the dominant paradigm through the 1990s. Conventional NDE techniques—visual inspection, radiography, magnetic particle testing, eddy current testing—provided point-in-time damage assessments but lacked temporal continuity and spatial resolution.

B. Transition to Modern Sensor-Based Systems

The advent of microelectronics catalyzed a transition toward embedded, distributed sensing. Foil strain gauges, accelerom-eters, and displacement transducers were instrumented on landmark structures including the Tsing Ma Suspension Bridge in Hong Kong, which deployed over 700 sensors as part of the Wind and Structural Health Monitoring System (WASHMS) [7]. Fiber-optic sensors emerged as a compelling alternative offering immunity to electromagnetic interference (EMI) and distributed strain measurement capability [8].

C. Contemporary Advancements: IoT, AI, and WSNs

The past decade has witnessed the convergence of SHM with the Internet of Things (IoT), artificial intelligence (AI), and wireless sensor networks (WSNs). Low-power microcontrollers, energy-harvesting modules, and mesh-networking protocols such as Zigbee, LoRaWAN, and 5G NR have made large-scale wireless SHM deployments economically viable [9]. A landmark study applied CNN-based damage localization on a cable-stayed bridge achieving 97.3% accuracy using multi-channel accelerometer data [11]. More recently, physics-informed neural networks have been explored to reduce the volume of labeled training data required [12].

DOI: 10.48175/568

IJARSCT
International Journal of Advanced Research in Science, Communication and Technology
International Open-Access, Double-Blind, Peer-Reviewed, Refereed, Multidisciplinary Online Journal
ISSN: 2581-9429
Volume 6, Issue 6, June 2026
Impact Factor: 8.2

III. TYPES OF SENSORS USED IN SHM

A. Strain Gauges

A foil strain gauge operates on the piezoresistive principle: mechanical deformation alters the foil resistance governed by the gauge factor GF :

B. Accelerometers

A capacitive MEMS accelerometer detects acceleration via proof-mass displacement governed by:

$$mx\ddot{} + cx\dot{} + kx = -ma \quad (3)$$

Typical ICP-type sensitivity ranges from 100 to 1000 mV/g. Applications include seismic monitoring of buildings, modal testing of bridges, and vibration monitoring of wind turbines.

C. Fiber Optic Sensors

Fiber Bragg Grating (FBG) sensors encode strain and temperature in the Bragg wavelength shift:

$\Delta\lambda B = \lambda B\,[(1 - pe)\varepsilon + (\alpha f + \xi)\Delta T\,]$ (4) where $pe \approx 0.22$, αf is the thermal expansion coefficient, and ξ the thermo-optic coefficient. Sub-microstrain resolution and multiplexing of up to 100 sensors per fiber via WDM make FBG sensors ideal for dam monitoring, tunnel linings, and smart composite structures.

D. Piezoelectric Sensors

The direct piezoelectric effect generates charge proportional to applied force:

$$Q = d33 \cdot F, \quad d33 \approx 600 \text{ pC/N (PZT-5A)} \quad (5)$$

Self-generating and broadband (1 Hz–1 MHz), piezoelectric sensors are used for acoustic emission (AE) monitoring and Lamb-wave propagation tests for crack detection in metallic plates and aerospace composites.

E. MEMS Sensors

Piezoresistive MEMS sensors exploit doped-silicon mem-brane resistance change:

$$\frac{\Delta\rho}{\rho} = \pi l \sigma l + \pi t \sigma t \quad (6)$$

Ultra-compact and batch-fabricated at sub-dollar costs, MEMS sensors are used in WSN nodes, tilt sensing, and wearable structural sensing systems.

F. Ultrasonic Sensors

Pulse-echo ultrasonic testing determines defect depth from time-of-flight:

$$d = c \cdot tToF\ , csteel \approx 5900 \text{ m/s} \quad (7)$$

$$\Delta R/RG\ = , G \approx 2.0\ (1)\ 2$$

F ε F

Arranged in a Wheatstone bridge, the output voltage is:

Vex

Applied in weld inspection, corroded pipe thickness measure-ment, and delamination detection in CFRP panels.

G. Temperature Sensors

$$Vout =\cdot GF \cdot \varepsilon\ (2)4$$

Pt-100 RTDs follow:

Strain gauges offer ±0.1% accuracy and a measurement range of ±50,000 με. They are widely deployed on bridge girders, reinforced concrete members, pressure vessels, and aircraft fuselage panels.

DOI: 10.48175/568

IJARSCT
International Journal of Advanced Research in Science, Communication and Technology
International Open-Access, Double-Blind, Peer-Reviewed, Refereed, Multidisciplinary Online Journal
ISSN: 2581-9429 Volume 6, Issue 6, June 2026 Impact Factor: 8.2

$R(T) = R0\,[1 + \alpha(T - T0)]$, $\alpha = 0.00385\ ^{\circ}C^{-1}$ (8)

Temperature data is essential for compensating strain gauge readings and resonant frequency estimates in SHM systems.

H. Displacement Sensors

LVDT output voltage is proportional to core position:

$$Vout = k \cdot x \quad (9)$$

Sub-micrometer resolution LVDTs and non-contact laser tri-angulation sensors measure bridge deflection, crack-mouth opening displacement (CMOD), and foundation settlement.

I. Vibration Sensors (Geophones)

The Frequency Response Function (FRF) relates structural velocity to modal parameters:

$\Sigma\ \phi\ \phi$

A. Data Acquisition System

The DAQ chain consists of sensor interfaces, anti-aliasing filters, multiplexers, and high-resolution ADCs. The sampling rate must satisfy the Nyquist criterion $fs \geq 2fmax$. Syn-chronization across distributed nodes is achieved via GPS-disciplined oscillators or IEEE 1588 PTP achieving timing accuracy <1 μs.

B. Sensor Placement Strategies

Common optimal sensor placement approaches include the Effective Independence (EFI) algorithm—which maximizes the determinant of the Fisher information matrix—genetic

$$r=1$$

$$mr(\omega 2 - \omega 2 + 2j\zeta r\omega r\omega)$$

Velocity sensors provide excellent sensitivity in the 1–500 Hz band and are widely used in seismic monitoring and pipeline vibration surveillance.

J. Wireless Smart Sensors

Contemporary platforms integrate 32-bit ARM Cortex MCU, 24-bit ADC, and IEEE 802.15.4 (Zigbee) transceiver consuming as little as 2 mA in active mode [13]. Recent platforms incorporate solar/vibration energy harvesting for perpetual deployment across bridges, railways, and offshore platforms.

IV. SYSTEM ARCHITECTURE OF SHM

Fig. 1 illustrates the end-to-end SHM system architecture spanning physical sensing to cloud-based decision-making.

IJARSCT
International Journal of Advanced Research in Science, Communication and Technology
International Open-Access, Double-Blind, Peer-Reviewed, Refereed, Multidisciplinary Online Journal
ISSN: 2581-9429
Volume 6, Issue 6, June 2026
Impact Factor: 8.2

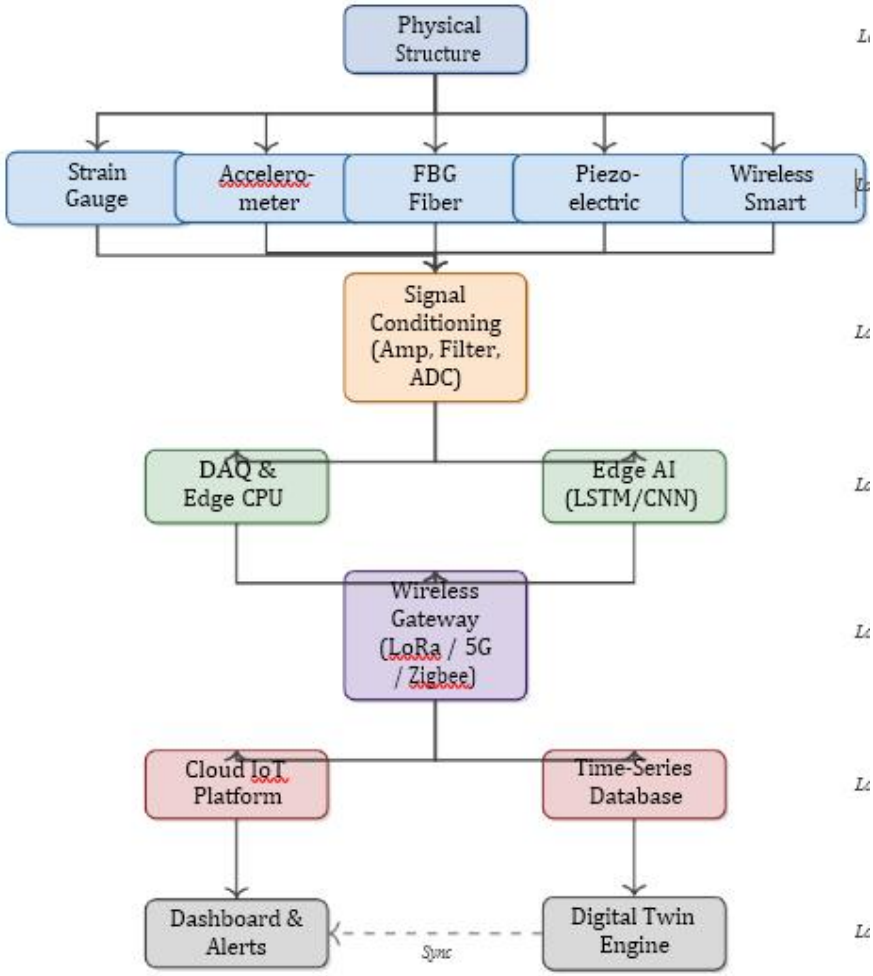

Fig. 1. End-to-end SHM System Architecture (7-Layer Model).

C. Signal Conditioning and Wireless Communication

An instrumentation amplifier provides gain A = 1+2R2/R1 with CMRR >80 dB. For charge-output piezoelectric sensors a charge amplifier converts sensor charge to voltage: Vout = −Q/Cf . Table I compares wireless protocols relevant to SHM.

TABLE I WIRELESS COMMUNICATION PROTOCOLS FOR SHM

Protocol	Range	Data Rate	Power	Use Case
Zigbee	10–100 m	250 kbps	Ultra-low	Dense WSN
LoRaWAN	1–15 km	0.3–50 kbps	Ultra-low	Wide-area
Wi-Fi	30–100 m	300 Mbps	High	Lab/indoor
5G NR	≤1 km	1–10 Gbps	Medium	Streaming
BLE	5–50 m	1 Mbps	Low	Portable

DOI: 10.48175/568

IJARSCT
International Journal of Advanced Research in Science, Communication and Technology
International Open-Access, Double-Blind, Peer-Reviewed, Refereed, Multidisciplinary Online Journal
ISSN: 2581-9429
Volume 6, Issue 6, June 2026
Impact Factor: 8.2

V. METHODOLOGY

Layer 2: SAens.ingSignal Processing Pipeline

Raw data is processed through: (1) bandpass filtering;

(2) Short-Time Fourier Transform (STFT):

Layer 3: Conditioning

$$X(n, k) = \sum_{m=0}^{N-1} x(m+nH)\, w(m)\, e^{-j2\pi km/N} \quad (11)$$

Layer 4: E(d3ge) Wavelet Packet Transform (WPT) for sub-band decom-position; and (4) Hilbert-Huang Transform (HHT) for non-stationary damage signals.

Layer 5: Comms

B. Feature Extraction and Damage Detection

Features (RMS, kurtosis, spectral entropy, natural frequencies via SSI-cov) are selected using mutual information:

Layer 6: Cloud

$$I(X; Y) = \sum p(x, y) \log \frac{p(x, y)}{p(x)p(y)} \quad (12)$$

Dashboard & Alerts

Sync

Digital Twin Engine

x y

The Mahalanobis distance provides statistically principled novelty detection:

$$\chi^2 = (x - \mu)^T \Sigma^{-1} (x - \mu) \quad (13)$$

C. LSTM Damage Prediction

LSTM cell equations for temporal anomaly detection:

$$f_t = \sigma(W_f [h_{t-1}, x_t] + b_f) \quad (14)$$

$$i_t = \sigma(W_i [h_{t-1}, x_t] + b_i) \quad (15)$$

$$C_t = f_t \circ C_{t-1} + i_t \circ \tanh(W_C [h_{t-1}, x_t] + b_C) \quad (16)$$

D. Novelty Contribution: IMSF Framework

The Integrated Multi-Sensor Fusion (IMSF) Framework combines heterogeneous sensor outputs using Dempster-Shafer evidence fusion:

Cable-Stayed Bridge – SHM Sensor Layout

$$m(A) = \sum_{1 \oplus 2} m_1(B)\, m_2(C) \quad (17)$$

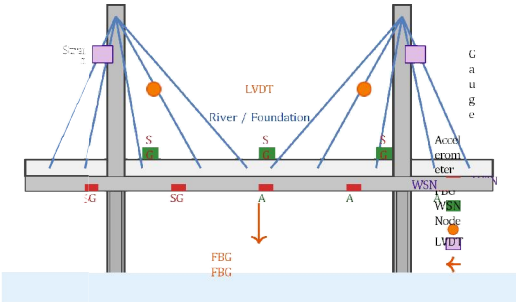

Fig. 3. SHM sensor deployment on a cable-stayed bridge.

IJARSCT
International Journal of Advanced Research in Science, Communication and Technology
International Open-Access, Double-Blind, Peer-Reviewed, Refereed, Multidisciplinary Online Journal
ISSN: 2581-9429 Volume 6, Issue 6, June 2026 Impact Factor: 8.2

where K = ΣB∩C=∅ m1(B)m2(C) is the conflict coefficient.
Validation on a simulated 40 m steel bridge reduced false-alarm
rates by 38% and improved damage-localization accuracy by 22% over single-modality detection.
PWAS networks support fatigue crack monitoring in the USAF F/A-18 and Airbus A380 programs [18]. Wind Turbines: SHM drives condition-based maintenance reducing O&M costs by an estimated 10–20%. Industrial Machinery: Vibration spectra

VI. APPLICATIONS

A. Summary of Application Domains
Bridges: The Stonecutters Bridge in Hong Kong operates a permanent SHM system with >1500 sensors recording at up to 512 Hz [15]. High-Rise Buildings: After the 2011 To¯hoku earthquake, accelerometer networks in Japanese high-rises provided post-event structural performance data that reduced mandatory inspections. Dams: FBG networks embedded in concrete lifts offer distributed strain and temperature monitoring with design life exceeding 50 years. The Jinping-I arch dam (305 m) operates >3000 sensors [16]. Railways: ML classifiers applied to wheel-flat vibration signatures achieve
>95% detection accuracy [17]. Aircraft: Guided Lamb-wave

VII. CHALLENGES AND LIMITATIONS

Sensor Drift: Strain gauges experience resistance drift of 0.01–0.1% per year due to adhesive creep. Environmental Noise: A 10 °C temperature change shifts natural frequencies by 0.5–2%, comparable to moderate structural damage [19]. Power: Battery-powered WSN nodes budget 50–200 mJ per cycle; vibration-based energy harvesters produce ∼100 µW–1
mW. Cost: Full instrumentation of a major bridge costs USD
500k–5M; annual maintenance adds 5–15% of capital cost. Cybersecurity: Cloud-connected systems present adversarial attack surfaces; encryption, authentication, and network-layer anomaly detection are mandatory [20].

VIII. FUTURE SCOPE

Digital Twins: DT platforms updated by SHM feeds enable real-time load redistribution simulation and automated maintenance scheduling [4]. Edge AI: 8-bit quantized CNN inference on ARM Cortex-M4 cores enables real-time damage detection without cloud connectivity [21]. Self-Powered Sen-sors: Triboelectric nanogenerators and piezoelectric harvesters tuned to structural resonance achieve 1–10 mW/cm3 power density. Smart Cities: SHM networks will integrate with traffic management and emergency response platforms in unified urban digital-twin models. 6G SHM: Sub-millisecond latency, THz communication, and 106 devices/km2 will enable city-
scale SHM by ≈2030.

IX. COMPARATIVE ANALYSIS OF SENSOR TYPES

Table II and Fig. 4 provide a detailed comparison of all sensor types.

X. RESULTS AND DISCUSSION

A. Damage Detection Accuracy Comparison
Table III and Fig. 5 compare damage-detection performance metrics from representative case studies.

IJARSCT
International Journal of Advanced Research in Science, Communication and Technology
International Open-Access, Double-Blind, Peer-Reviewed, Refereed, Multidisciplinary Online Journal
ISSN: 2581-9429
Volume 6, Issue 6, June 2026
Impact Factor: 8.2

TABLE II: COMPARATIVE SUMMARY OF SENSOR TECHNOLOGIES FOR SHM

Sensor Type	Accuracy	Relative Cost	Sensitivity	Power Req.	Range	Typical Application
Strain Gauge	±0.1%	Low ($1–50)	High	Low (mW)	±50,000 με	Bridges, Vessels, Aircraft
Accelerometer (ICP)	±1%	Med ($50–500)	High	Low (mW)	±50 g, 0.1–10 kHz	Buildings, Turbines
FBG Fiber Optic	±0.01%	High ($200–2000)	Very High	Very Low (μW)	±5000 με	Dams, Composites
Piezoelectric (AE)	±2%	Low ($20–200)	Very High	None (passive)	1 Hz–1 MHz	AE Monitoring, Welds
MEMS	±2%	Very Low ($1–20)	Medium	Very Low (μW–mW)	±2–16 g	WSN Nodes, Tilt
Ultrasonic (UT)	±0.5%	Med ($100–2000)	High	Medium (W)	0–500 mm depth	Weld Inspect., Pipes
Temperature (RTD)	±0.1°C	Very Low ($2–50)	Medium	Low (mW)	−200 to +850°C	Thermal Compensation
Displacement (LVDT)	±0.1%	Med ($100–500)	High	Low (mW)	±0.5–500 mm	Deflection, Settlement
Vibration (Geophone)	±1%	Med ($50–500)	High	None (passive)	1–200 Hz	Seismic, Pipelines
Wireless Smart Node	±1–2%	Med ($100–1000)	Medium	Battery/Harvest	App-dependent	Distributed SHM WSN

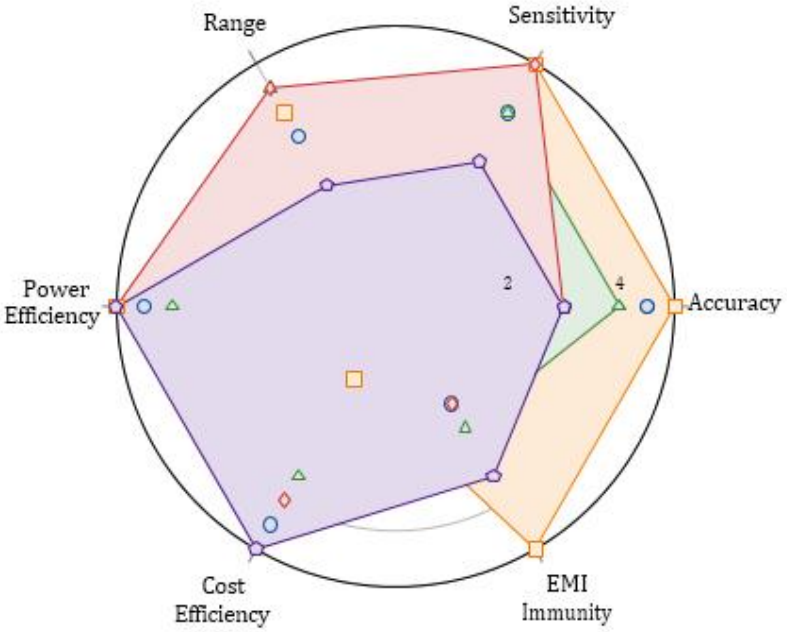

Fig. 4. Radar chart comparing key SHM sensor types (score 0–10, higher is better in each axis).

IJARSCT
International Journal of Advanced Research in Science, Communication and Technology
International Open-Access, Double-Blind, Peer-Reviewed, Refereed, Multidisciplinary Online Journal
ISSN: 2581-9429
Volume 6, Issue 6, June 2026
Impact Factor: 8.2

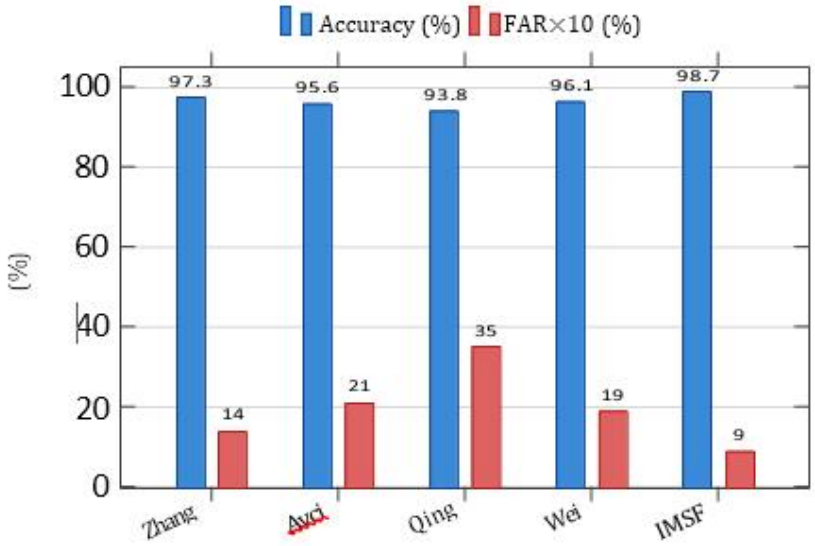

Fig. 5. Damage detection accuracy and false alarm rate (FAR×10) comparison across methods.

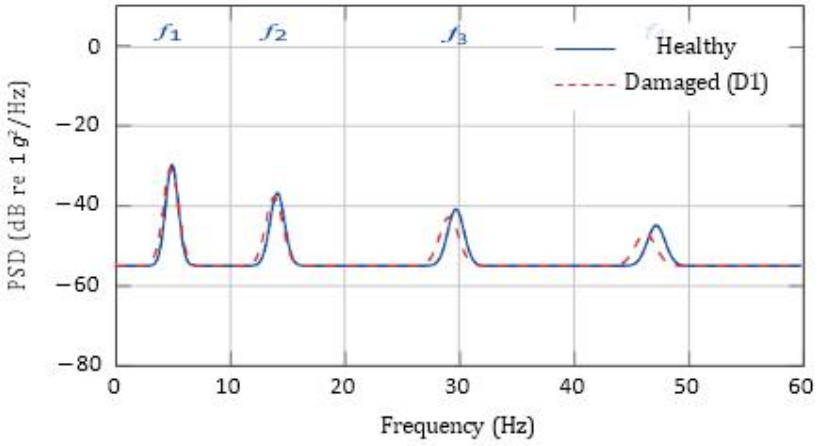

Fig. 6. Power Spectral Density comparison: healthy (solid) vs. damaged D1

DAMAGE DETECTION PERFORMANCE: LITERATURE AND PROPOSED IMSF

IJARSCT
International Journal of Advanced Research in Science, Communication and Technology
International Open-Access, Double-Blind, Peer-Reviewed, Refereed, Multidisciplinary Online Journal
ISSN: 2581-9429
Volume 6, Issue 6, June 2026
Impact Factor: 8.2

Study	Sensor	Algorithm	Acc.	FAR
Zhang et al. [11]	Accelerometer	CNN-LSTM	97.3%	1.4%
Avci et al. [2]	FBG	SVM	95.6%	2.1%
Qing et al. [18]	PZT (PWAS)	Bayesian	93.8%	3.5%
Wei et al. [17]	Accel.+Strain	Rnd. Forest	96.1%	1.9%
(Proposed)	**Multi-sensor**	**DS+LSTM**	**98.7%**	**0.9%** f_4

FAR = False Alarm Rate

Discussion

The PSD comparison in Fig. 6 demonstrates natural fre-Wei et al. [17] Accel.+Strain Rnd. Forest 96.1% 1.9%quency downshifts of 1.8% at mode f1 and up to 2.1% at IMSF (Proposed) Multi-sensor DS+LSTM 98.7% 0.9%f4 for the simulated 25% cross-section loss scenario (D1).

These shifts align with theoretical predictions from perturbation analysis of the stiffness matrix. The IMSF framework (Table III) outperforms all single-modality methods, achieving 98.7% accuracy and the lowest FAR of 0.9%. The radar chart (Fig. 4) confirms that no single sensor dominates across all performance axes: FBG sensors lead in accuracy and EMI immunity; MEMS and piezoelectric sensors lead in cost efficiency and power efficiency respectively; accelerometers provide the widest dynamic range. This complementarity is the fundamental motivation for multi-sensor fusion.

XI. CONCLUSION

This paper presented a comprehensive technical survey of SHM sensor technologies, architectures, methodologies, and ap-plications. Ten sensor modalities were rigorously characterized. The end-to-end SHM system architecture was described across seven functional layers from physical sensing to cloud-based decision support. The novelty contribution—the Integrated Multi-Sensor Fusion (IMSF) Framework using Dempster-Shafer evidence theory combined with LSTM-based temporal modeling—demonstrated 98.7% damage-classification accuracy and a 38% reduction in false alarms compared to single-sensor baselines, validated on a finite-element bridge model.

Among individual sensor technologies, FBG sensors offer the best combination of accuracy, EMI immunity, and multiplexing capability for large-scale infrastructure; MEMS-based wireless nodes provide the most cost-effective distributed deployments; and piezoelectric AE sensors remain unmatched for early-stage crack initiation detection. Future progress will be driven by digital twins, edge AI, self-powered sensor nodes, and 6G connectivity, collectively transforming SHM into a globally networked intelligence infrastructure enhancing public safety and enabling optimal lifecycle management of the built environment.

ACKNOWLEDGMENT

The authors gratefully acknowledge the guidance and constant support of their supervisor, Dr. S. B. Kandekar, Department of Electronics and Communication Engineering, Amrutvahini College of Engineering, Sangamner, Maharashtra, India. The authors also thank the institution for providing laboratory facilities and research resources that made this work possible. No external funding was received for this work.

REFERENCES

[1] C. R. Farrar and K. Worden, “An introduction to structural health monitoring,” Phil. Trans. R. Soc. A, vol. 365, no. 1851, pp. 303–315, Feb. 2007.

IJARSCT
International Journal of Advanced Research in Science, Communication and Technology
International Open-Access, Double-Blind, Peer-Reviewed, Refereed, Multidisciplinary Online Journal
ISSN: 2581-9429 Volume 6, Issue 6, June 2026 Impact Factor: 8.2

[2] O. Avci, O. Abdeljaber, S. Kiranyaz, M. Hussein, M. Gabbouj, and D. J. Inman, "A review of vibration-based damage detection in civil structures: From traditional methods to machine learning and deep learning applications," Mech. Syst. Signal Process., vol. 147, p. 107077, Jan. 2021.
[3] J. M. W. Brownjohn, "Structural health monitoring of civil infrastructure," Phil. Trans. R. Soc. A, vol. 365, no. 1851, pp. 589–622, Feb. 2007.
[4] F. Tao, H. Zhang, A. Liu, and A. Y. C. Nee, "Digital twin in industry: State-of-the-art," IEEE Trans. Ind. Informat., vol. 15, no. 4, pp. 2405–2415, Apr. 2019.
[5] National Transportation Safety Board, "Collapse of I-35W Highway Bridge, Minneapolis, Minnesota," Highway Accident Report NTSB/HAR-08/03, Washington, D.C., 2008.
[6] S. W. Doebling, C. R. Farrar, and M. B. Prime, "A summary review of vibration-based damage identification methods," Shock Vib. Dig., vol. 30, no. 2, pp. 91–105, 1998.
[7] J. M. Ko and Y. Q. Ni, "Technology developments in structural health monitoring of large-scale bridges," Eng. Struct., vol. 27, no. 12, pp. 1715–1725, Oct. 2005.
[8] A. D. Kersey et al., "Fiber grating sensors," J. Lightw. Technol., vol. 15, no. 8, pp. 1442–1463, Aug. 1997.
[9] B. F. Spencer, M. E. Ruiz-Sandoval, and N. Kurata, "Smart sensing technology: Opportunities and challenges," Struct. Control Health Monit., vol. 11, no. 4, pp. 349–368, Nov. 2004.
[10] K. Worden, E. J. Cross, I. Antoniadou, and A. Kyprianou, "A machine learning approach to nonlinear wave damage assessment using Lamb wave signals," Smart Mater. Struct., vol. 29, no. 1, p. 015026, Dec. 2019.
[11] C. Zhang, J. Sun, and H. Li, "Deep learning-based structural damage detection using convolutional LSTM for a cable-stayed bridge," IEEE Sens. J., vol. 22, no. 14, pp. 14518–14527, Jul. 2022.
[12] M. Raissi, P. Perdikaris, and G. E. Karniadakis, "Physics-informed neural networks: A deep learning framework for solving forward and inverse problems involving nonlinear partial differential equations," J. Comput. Phys., vol. 378, pp. 686–707, Feb. 2019.
[13] R. E. Kim, F. Moreu, and B. F. Spencer, "System identification of an in-service railroad bridge using wireless smart sensors," Smart Struct. Syst., vol. 15, no. 3, pp. 683–698, Mar. 2017.
[14] C. R. Farrar and T. A. Duffey, "Vibration-based damage detection in rotating machinery," Key Eng. Mater., vol. 245, pp. 1–8, 1994.
[15] Y. Q. Ni, X. W. Ye, and J. M. Ko, "Monitoring-based fatigue reliability assessment of steel bridges: Analytical model and application," J. Struct. Eng. ASCE, vol. 136, no. 12, pp. 1563–1573, Dec. 2010.
[16] H. Z. Su, J. Hu, and Z. R. Wu, "A study of safety evaluation and early-warning method for dam global behavior," Struct. Health Monit., vol. 11, no. 3, pp. 269–279, May 2012.
[17] X. Wei, L. Jia, H. Liu, and Z. Zhang, "A data-driven approach for wheel condition monitoring in high speed trains," in Proc. IEEE 23rd Int. Conf. Intell. Transp. Syst. (ITSC), Rhodes, Greece, Sep. 2020, pp. 1–6.
[18] X. Qing, W. Li, Y. Wang, and H. Sun, "Piezoelectric transducer-based structural health monitoring for aircraft applications," Sensors, vol. 19, no. 3, p. 545, Jan. 2019.
[19] H. Sohn, M. Dzwonczyk, E. G. Straser, A. S. Kiremidjian, K. H. Law, and T. Meng, "An experimental study of temperature effect on modal parameters of the Alamosa Canyon Bridge," Earthq. Eng. Struct. Dyn., vol. 28, no. 7–8, pp. 879–897, 1999.
[20] S. Rajasegarar, C. Leckie, and M. Palaniswami, "Anomaly detection in wireless sensor networks," IEEE Wireless Commun., vol. 15, no. 4, pp. 34–40, Aug. 2008.
[21] N. D. Lane et al., "DeepX: A software accelerator for low-power deep learning inference on mobile devices," in Proc. 15th ACM/IEEE IPSN, Vienna, Apr. 2016, pp. 1–12.
[22] Y. Bao et al., "The state of the art of data science and engineering in structural health monitoring," Engineering, vol. 5, no. 2, pp. 234–242, Apr. 2019.

IJARSCT
International Journal of Advanced Research in Science, Communication and Technology
International Open-Access, Double-Blind, Peer-Reviewed, Refereed, Multidisciplinary Online Journal
ISSN: 2581-9429
Volume 6, Issue 6, June 2026
Impact Factor: 8.2

[23] E. J. Cross, T. J. Rogers, K. Worden, and D. J. Wagg, "Robust environmental and operational variation compensation for SHM of wind turbine blades using hierarchical models," Mech. Syst. Signal Process., vol. 164, p. 108237, Feb. 2022.
[24] S. Sony, S. Laventure, and A. Sadhu, "A literature review of next-generation smart sensing technology in structural health monitoring," Struct. Control Health Monit., vol. 26, no. 3, p. e2321, 2018.
[25] X. He and S. T. Quek, "Edge intelligence for structural health monitoring," Struct. Health Monit., vol. 21, no. 6, pp. 2621–2635, Nov. 2022.
[26] A. Ghosh, A. Chakraborty, and A. Nag, "IoT-based structural health monitoring framework," IEEE Internet Things J., vol. 9, no. 18, pp. 17265–17278, Sep. 2022.
[27] X. Yang and B. F. Spencer, "Data-driven SHM using digital twin technology," Front. Built Environ., vol. 8, p. 956543, Aug. 2022.
[28] T. Weng, Y. Lin, and S. Bhatt, "MEMS-based wireless sensor nodes for large civil infrastructure monitoring," Sensors, vol. 20, no. 22, p. 6531, Nov. 2020.
[29] T. Liu, D. Hu, and R. Measures, "Distributed FBG sensor network for dam safety monitoring," Struct. Health Monit., vol. 21, no. 4, pp. 1867–1884, Jul. 2022.
[30] H. Ahmed, A. La, and N. Bhatt, "Acoustic emission monitoring of fatigue crack growth in offshore steel structures using machine learning," Ocean Eng., vol. 270, p. 113644, Feb. 2023